Article:
Bradley, D., Palacios, A. and Hu, L. (Cover date: December 2023) Blow-off of Fuel Jet Flames in the Atmosphere. Fire Safety Journal, 141. 104007. ISSN: 0379-7112

https://doi.org/10.1016/j.firesaf.2023.104007

Blow-off of Fuel Jet Flames in the Atmosphere

Adriana Palacios[1,*], Derek Bradley[2], Longhua Hu[3]

[1]*Universidad de las Americas, Puebla, Department of Chemical, Food and Environmental Engineering, Puebla, Mexico.*
[2]*University of Leeds, School of Mechanical Engineering, Leeds, UK.*
[3]*State Key Laboratory of Fire Science, University of Science and Technology of China.*
**Corresponding author's email: adriana.palacios@udlap.mx*

Abstract

Further data from experiments with the atmospheric burning of jet fuels, particularly their blow-off and flame quenching characteristics, have been collected and interpreted. These are characterised in terms of both their dimensionless Flow Number and Flame Thickness. Regimes of Lifted Flames, Flame Blow-off, Choked Flow and Flame Quench have been defined by these Dimensionless Groups. New data are presented for a variety of hydrocarbon and ammonia-hydrogen fuels. New techniques are required for the assessment of the latter, including derivation of their acoustic velocities and the characterisation of their laminar flames, including burning velocity and flame thickness. It is possible to create NH_3+H_2 jet flow blends with burning rates and blow-off velocities that are closer to those of hydrocarbons than of H_2. The properties of individual fuels are displayed in terms of the fuel velocities at which blow-off occurs for different pipe diameters. The properties of individual fuels displayed in this way show a greater diversity than is evident from the dimensionless groups. Similarities are drawn between premixed and jet flow flame quenching.

Keywords: jet flames; blow-off; NH_3+H_2 blends; hydrocarbons.

Nomenclature

a acoustic velocity at pipe exit plane (m/s)
Cp specific heat at constant pressure (kJ/kmole· °C), at *T* or (J/kg· K), at T^o
Cv specific heat at constant volume (kJ/kmole· °C), at *T*
D pipe diameter (m) or (mm)
k thermal conductivity (W/m· K) at T^o
M Mach number at pipe exit plane, (u_j/a_j)
MW Molecular weight (kg/kmol)
P_a atmospheric pressure (Pa)
P_i initial stagnation pressure (Pa)
R mass specific gas constant equal to the Universal Gas constant of 8314 J/kmol· K
S_L maximum laminar burning velocity of the fuel air mixture at ambient atmosphere (m/s)
T ambient temperature (K)
T^o temperature at inner layer of laminar flame (K)
u fuel flow velocity at exit plane of burning jet fuels supply pipe (m/s)
U^* dimensionless Flow Number for choked and unchoked flow, $(u_j/S_L)(\delta_k/D)^{0.4}(P_i/P_a)$
U_b^* U^* value at blow-off
X molar fraction
X_a ammonia fuel molar fraction in the fuel mixture

Greek

δ_k flame thickness, $(k/Cp)T_o/\rho_u S_L$ (m), Eq. (1)
γ ratio of specific heats
ρ density (kg/m^3)

Subscripts

a ambient conditions
b blow-off conditions
i initial stagnation conditions
j pipe exit plane
u unburned gas
1 gas 1
2 gas 2

1. Introduction

The paper deals with the blow-off of atmospheric jet flames from the end of fuel pipes, usually of circular cross-section. The origins of the work are the culmination of both lengthy mathematical modelling of fuel flame blow-off, and compilations of the experimental data of the phenomena. In [1] a dimensionless flow number, U^*, is introduced, with which jet flame heights and lift-off distances have been correlated. The fuel blow-off velocity, u, is that of the gaseous fuel at the exit plane of the pipe, ahead of the flame. A dimensionless Flow Number, U^*, is defined by:

$$U^* = (u/S_L)\,(\delta_k D)^{0.4}(Pi/Pa). \qquad (1)$$

Fuel properties are expressed through its maximum laminar burning velocity with air, S_L, and its laminar flame thickness, δ_k, normalised by the pipe diameter, D. Hydrogen and hydrocarbon thermo- physical and isentropic expansion data were obtained from the GasEq Code [2].

The inclusion of S_L arose as a consequence of the computations showing that after fuel/air mixing in the fuel jet, reaction was predominantly in the most reactive zone, where the mixture had a laminar burning velocity, close to its maximum value [1]. For the avoidance of flame quenching, the ratio, $\delta k/D$, must be sufficiently small. The approach of Göttgens et al. [3] was employed, in the derivation of δk. This involved identifying an inner layer temperature, T^o, below which, no reaction occurs.

In the expression for U^* the initial stagnation to exhaust pressure ratio, (Pi/Pa), arising from the exit plane fuel velocity, u, is given by:

$$(Pi/Pa) = [(M^2(\gamma - 1) + 2)/2]^{\gamma/(\gamma - 1)}. \qquad (2)$$

In the case of mixed fuels, the physico-chemical parameters are those of the fuel blend. The black filled circular symbols in Fig. 1 are of CH_4+H_2 blends. In a study of hydrogenation of natural gas burners S_L values of such blends were obtained experimentally [4].

In [5], a general correlation of flame Blow-off and Quench, is expressed in terms of U^* and δ_k/D. This is demonstrated by the past and present experimental results in Fig. 1. A sufficiently high fuel velocity will lift the flame well clear of the burner, at a value, U_b,* and it will then blow-off. This upper regime of Flame Blow-off is indicated, as also can be the lower one of Lifted Flames.

The Blow-off boundary is indicated by the value, U_b*, which separates the regimes. Sonic fuel velocities can arise at the exit plane, as indicated by the dashed horizontal lines. Blow-off curves indicate, the values of U_b*. As the fuel jet velocity increases, more air is entrained. This can eventually become excessive, the flame blows off the pipe, and is quenched. Flame quenching at the fuel pipe rim occurs, at the higher values of δ_k/D at the Quench curves. The quench is induced by the increased relative cooling at low *D*, and is discussed further in Section 4.1. The Quench and Blow-off Boundary curves for C_3H_8, CH_4, and H_2, all form a continuum, tracing the transition from the onset of quenching to the development of blow-off. In contrast, an extreme, design example is that of the projected large-scale flaring is that might follow the venting of hydrogen from failed nuclear reactors, to avert a more serious explosion. In this instance a high hydrogen flow rate of 176.5 kg/h was necessary [6]. The coordinate conditions are given on Fig.1, low on the right.

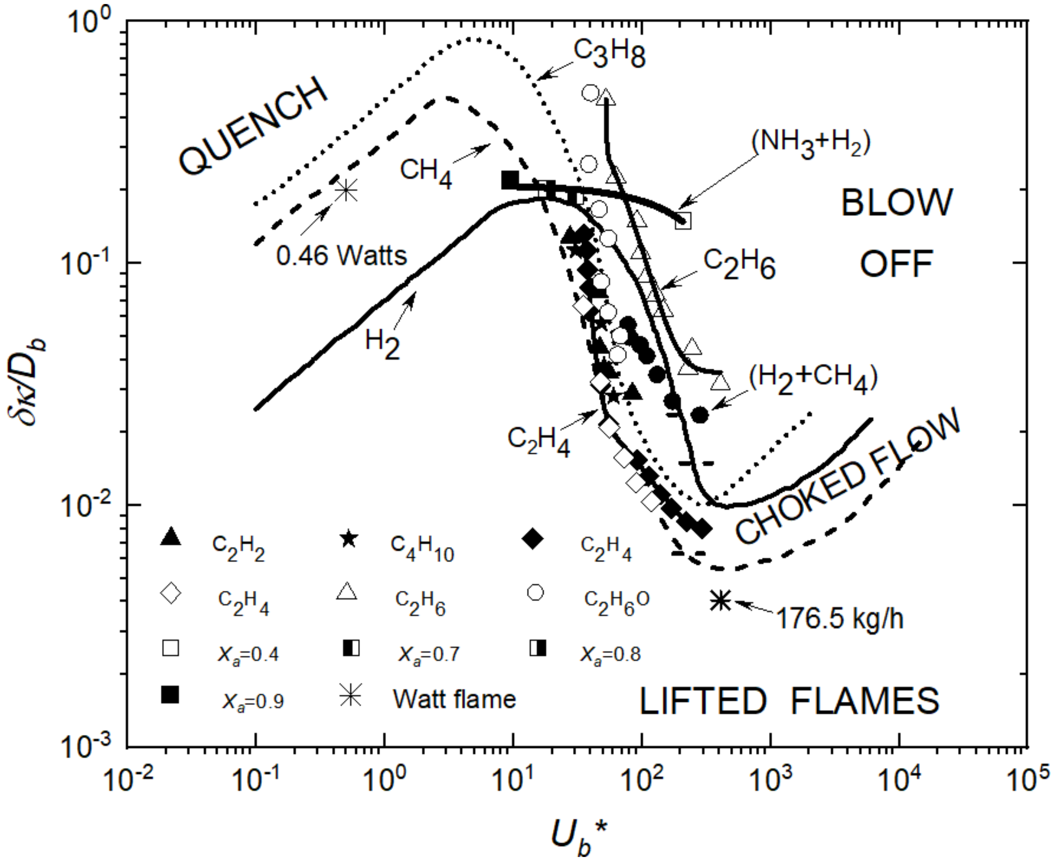

Fig. 1. Regimes of jet flame combustion of different fuels. The lines indicate both Quench and Blow-off boundaries, with the dashed horizontal lines indicating Choked Flow. The new data points are indicated by open symbols and, for NH_3+H_2, with variably filled squares.

2. New data

The present paper introduces new data from the additional fuels into Fig. 1. Experimental data points, from a variety of sources, listed in the References, have been correlated in the course of the present study, and the ranges of results appear in Table 1, as well as in Fig. 1. These new data points for the new fuels are indicated by the open symbols, and by variably filled squares for ammonia/H_2. Ethane [7], propane [5] and hydrogen [5] data yielded somewhat higher values of U_b*, while those for ethylene [7], and dimethyl ether [7] are somewhat lower. New burner diameters range between 1 and 14 mm. The ammonia- hydrogen mixtures [8] had NH_3 fuel mole fractions, X_a, of 0.4, 0.7, 0.8, 0.9. These are indicated by square symbols. If the ammonia proportion is rather low, the square is empty, if it is moderately low the left half is black, if moderately high the right half is black and if it is very high, it is completely black. Table 1 shows the ranges of the different new measurements.

Table 1. New experimental data for the derivation of values of $U*$ and δ_k/D.

Author (Year) [Reference]	Fuel	Pipe Diameter (*D*), mm	Blow-Off Velocity (*u*), m/s
Um et al. (2013) [8]	Ammonia-Hydrogen	2.7	15 – 125
Stamps and Tieszen (2014) [7]	Ethane	1 – 14	29 – 329
Stamps and Tieszen (2014) [7]	Ethylene	1 – 6	75 – 310
Stamps and Tieszen (2014) [7]	Dimethyl Ether	1 – 12	23 – 95

3. Treatment of (NH_3+H_2) mixtures

As a fuel, NH_3 has poor flammability, with a maximum atmospheric laminar burning velocity of only about 0.06 m/s, which is much less than the value of about 2.9 m/s for hydrogen. However, NH_3 is very effective as a liquefying agent for hydrogen. The stored energy density capabilities of liquified NH_3+H_2 are higher than those of, both batteries and hydrogen, alone [9]. With 40% NH_3 as a fuel blended with H_2, the laminar burning velocity has a more practical value of 0.8 m/s.

Um et al. [8] have measured the lift-off and blow-off jet velocities, *u*, of (NH_3+H_2) blends, for different NH_3 fuel fractions, X_a, in the range between 0 and 1, from a pipe of 2.7 mm diameter, *D*.

The necessary maximum laminar burning velocities of the fuel mixture, S_L, were obtained from the computed laminar burning velocities of Lhuillier et al. [10], again for different fractions of NH_3 in (NH_3+H_2) mixtures, at the different equivalence ratios. Flame thicknesses, in the absence of any guidance from [3], were taken from the generalised values collated by Lee et al. in [11]. Here, some computed values of the flame thickness are presented as a function of equivalence ratio and the stoichiometric fraction of the ammonia. It was necessary to extrapolate the given data to the present conditions. As the ammonia fraction in (NH_3+H_2), increased from 0.4 to 0.9, the laminar flame thickness, δ_k, increased from 0.4 to 0.6 mm. Rather tentative, values enabled the (NH_3+H_2) blow-off data of Um et al. [8] to be plotted in Fig. 1. More blow-off data over wider ranges of NH_3+H_2 blends and jet diameters are required to make this plot more definitive.

Evaluation of P_i/P_a, from Eq. (2), requires appropriate values of acoustic velocities, a, for the different ammonia-hydrogen concentrations, in order to determine the Mach number in the equation. Here the procedures followed those of Dixon and Greenwood [12]. For a single species, the acoustic velocity is found from:

$$a = (\gamma RT)^{0.5}, \quad (3)$$

with a value of R given by 8314 J/kmol· K, divided by the average molecular weight of the NH_3+H_2 mixture. The value of γ, the ratio of specific heats, is obtained for the mixtures of gases from the expression in [11]:

$$\gamma_{mixture} = \frac{Cp_1 \cdot X_1 + Cp_2 \cdot X_2}{Cv_1 \cdot X_1 + Cv_2 \cdot X_2}. \quad (4)$$

Here C_p and C_v are the specific heats at constant pressure and volume (J/kg· K), respectively, of the gases 1 and 2. Values of C_p and C_v were calculated at 25°C and 1 atm, for pure H_2 and pure NH_3, using the software, following Aspen-Hysys V10® [13]. These results, together with other data used for the calculation of a, through Eqs. (3-4), are shown in Table 2. These values were substituted into Eq. (4) to yield γ values for the NH_3+H_2 mixtures, for the different NH_3 and H_2 molar fractions, X_{NH3} and X_{H2} in the experiments.

The low ammonia concentration acoustic velocity for a particular NH_3+H_2 mixture, was found from Eq. (3). The calculated value of γ for the particular mixture was substituted into Eq. (3), together with the ambient temperature, T = 298.15 K, together with the value of R, which was then divided by the average molecular weight of the NH_3+H_2 blend. The highest ammonia blended fuel velocities were with X_a=0.4, with the maximum proportion of H_2. This gave a maximum P_i/P_a value of 1.03. With maximum NH_3, at X_a=0.9, and P_i/P_a=1.0006.

Table 2. Data used in Eqs. (3)-(4), obtained from the software Aspen-Hysys V10® [13].

Fuel	***Cv*** **(kJ/kmole·°C)**	***Cp*** **(kJ/kmole·°C)**	γ	***MW*** **(kg/kmol)**	***a*** **(m/s)**
Ammonia	27.41	35.69	1.3	17.03	437
Hydrogen	20.11	28.42	1.4	2.016	1314

4. Blow-off velocities for different fuels at different pipe diameters

Much detailed information concerning the blow-off of different fuels is concisely summarised by the dimensionless blow-off relationships of Fig. 1. To demonstrate some of the marked practical differences between fuels with regard to blow-off, the blow-off velocities at different pipe diameters were accessed. Each species retains its thermophysical properties. Values of U^* on the generalized curve and the corresponding values of $\delta k/D$ are noted. From the appropriate physico-chemical properties, S_L, δk, and a, the selected pairs of dimensionless groups yielded the fuel blow-off velocities, u, at the different values of pipe diameter for blow-off, D. Figure 2 shows the plots of values of u against these values of D for H_2, and also for three values of (NH_3+H_2), for different fractions of ammonia in the (NH_3+H_2) fuel mix.

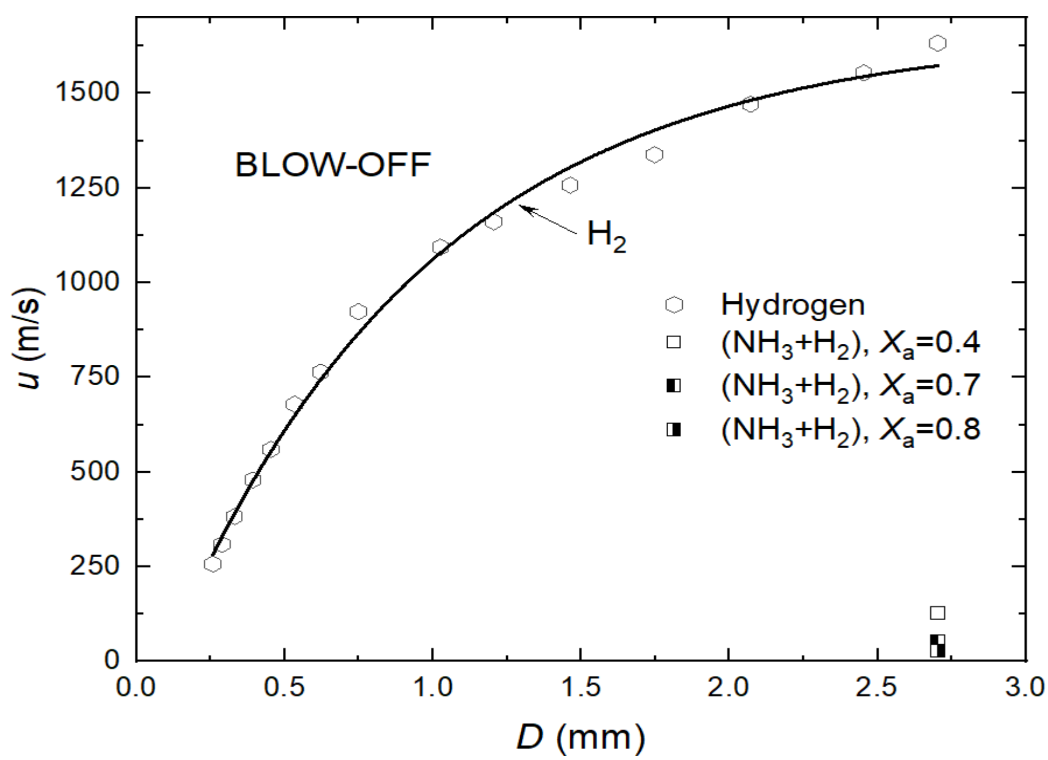

Fig. 2. Blow-off velocities and pipe diameters for NH_3+H_2 (X_a = 0.4-0.8) [8] and hydrogen jet flames [5].

Striking aspects are the high blow-off velocities that are attained with H_2 and shown in Fig. 2. These are associated with its high acoustic velocities, and contrast with the much lower values with the NH_3+H_2 mixture. Hydrogen flames can be sustained on exceptionally small diameter burners, whilst being able to operate with high velocities on higher diameter burners.

It can be seen from Fig. 3 that ethane and ethylene require higher diameter burners to sustain blow- off velocities, in both instances, of up to 300 m/s. Interestingly, in the case of ethane, at the lower values of *D*, the (NH_3+H_2) blends can attain similar jet velocities. With the relatively high proportion of H_2 at X_a=0.4, the blow-off velocity is relatively high and closer to that of ethylene than the ethane values. With the higher NH_3 content of X_a=0.7, the blow-off velocity is reduced, but is still close to that of ethane in Fig. 3, and might remain at larger values of *D*. The NH_3+H_2 blend, although limited experimentally in the present study, by just a single-valued *D*, has a greater affinity with the two hydrocarbons than with H_2, see Fig. 3.

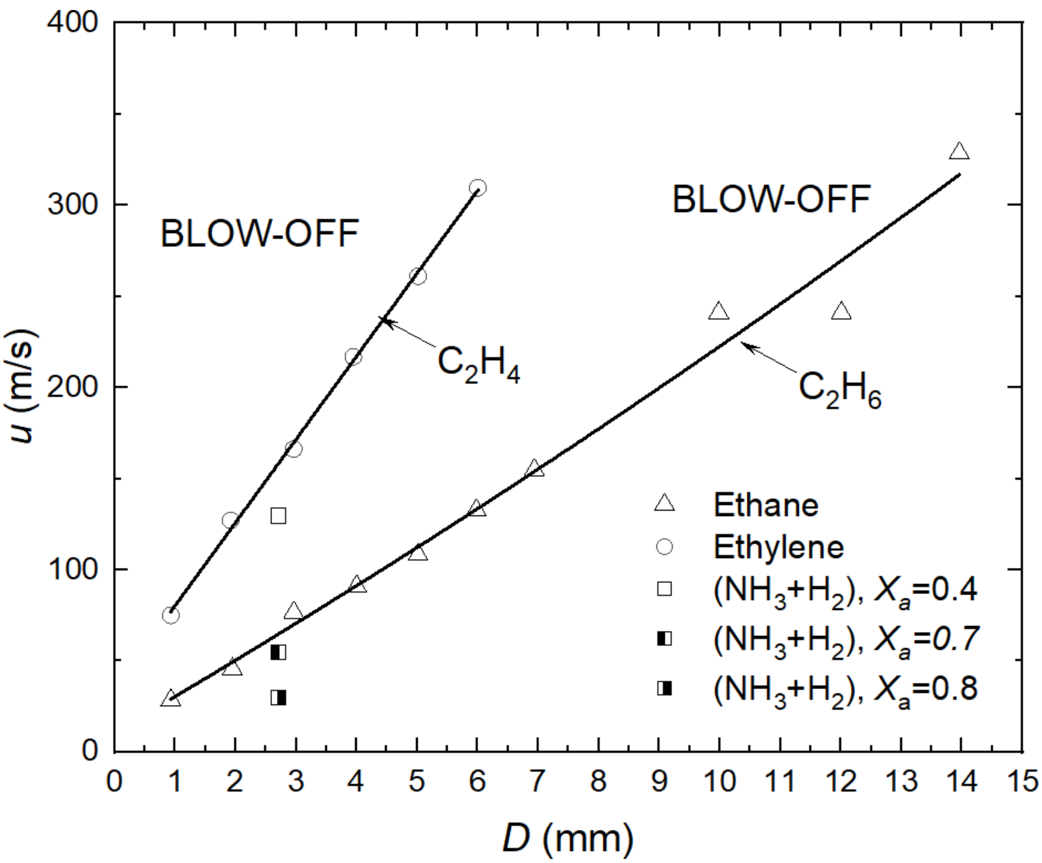

Fig. 3. Fuel jet flame Blow-off velocities, at different pipe diameters, for ethane [7], ethylene [7], and (NH_3+H_2) blends [8].

The performance of the two paraffins, CH_4 and C_3H_8, shown in Fig. 4, might be regarded as robust, even down to moderately small pipe diameters. This trend continues with the butane characteristics, shown in Fig. 5, but the more complex molecular structure of Di-methyl ether leads to a smaller fuel velocity that requires a greater pipe diameter.

Figures 2 to 5 display a greater diversity in the different fuel characteristics than is apparent from Fig.1. It can be seen that blow-off velocities increase with increasingly higher paraffins. Jet flames can arise in a variety of circumstances, on burners, engines and a diverse flare [14], with almost a hundred-fold range in their heat release rates.

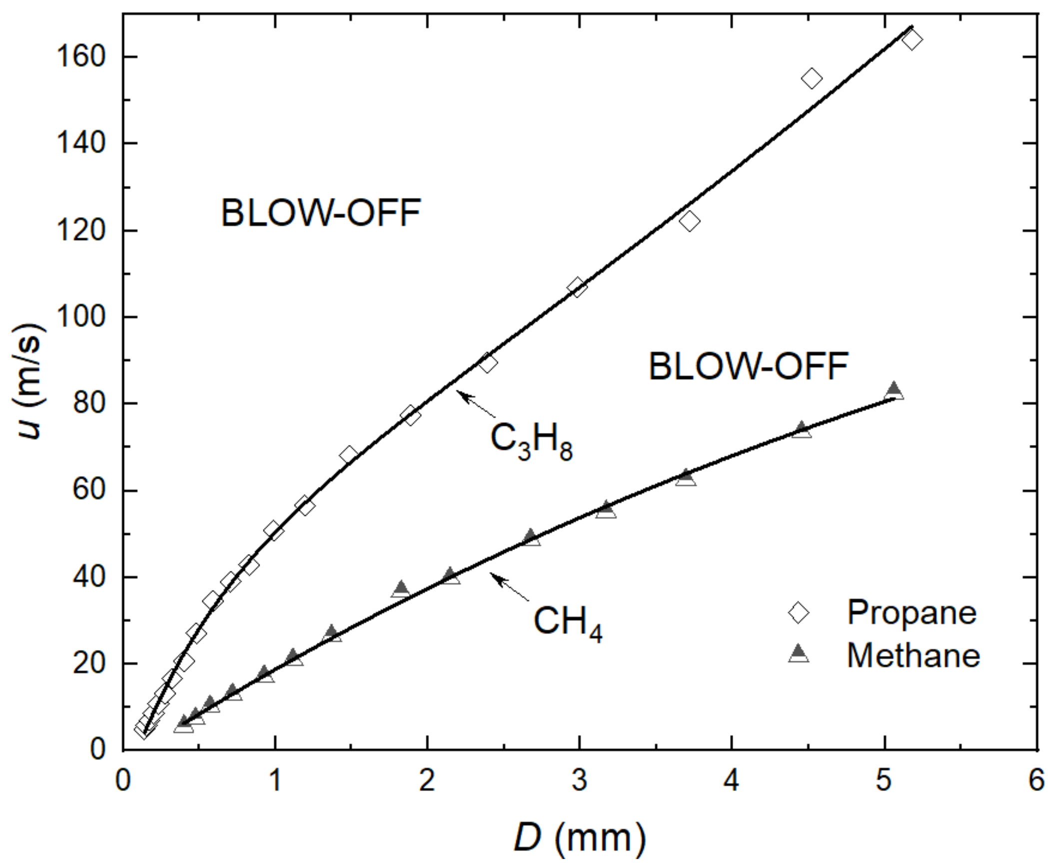

Fig. 4. Fuel jet flame Blow-off velocities at different pipe diameters for methane and propane jet flames [5].

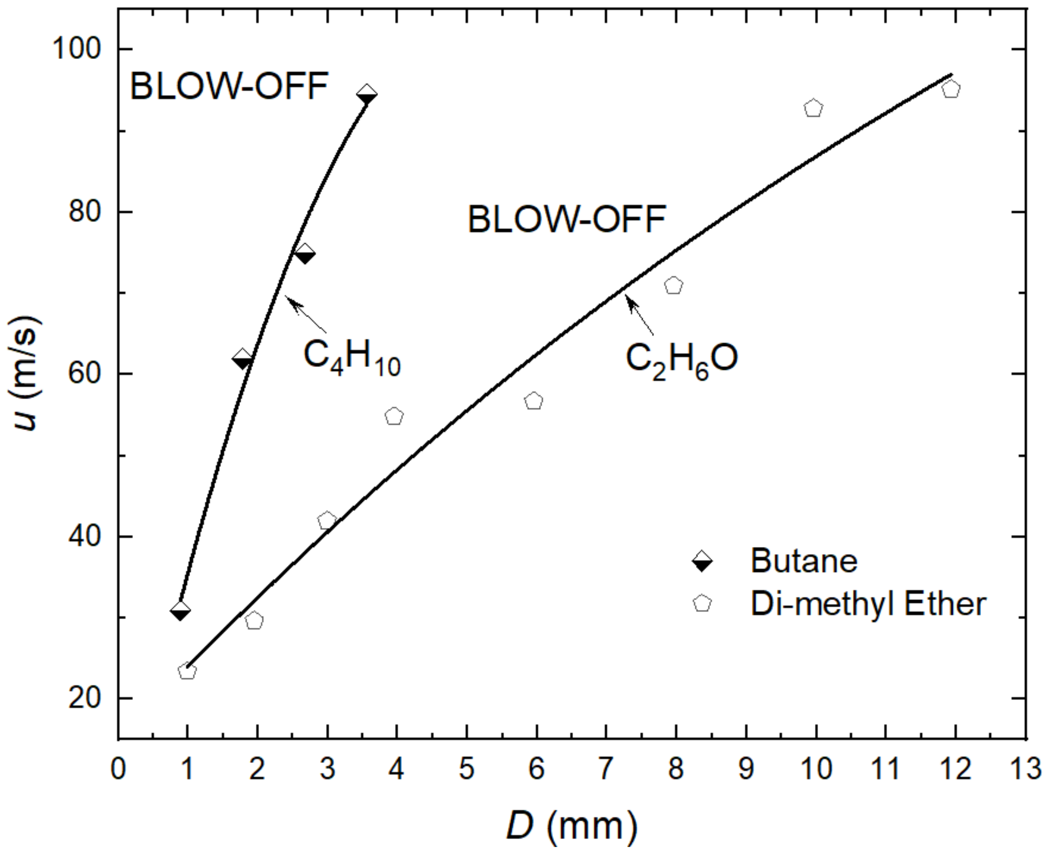

Fig. 5. Fuel jet flame Blow-off velocities at different pipe diameters for butane [5] and Di-methyl ether [7] jet flames.

4.1. Low burn rates and flame quench

A high energy release rate of a fuel is not necessarily optimal practically, and the use of ammonia to "slow down" the reaction rate of H_2 can be just as valuable. The flame quenching mechanism is very similar to that associated with the flame quenching premixed flames. In both instances the small eddies cannot survive the combination of a high strain rate and excessive heat loss. A swinging laser sheet experimental technique [14] was employed to study the quenching of small premixed flame kernels with a variety of fuels. This revealed a close similarity of such extinctions with the quenching that ensued after the blow-off of different fuel jet flames from small diameter pipes. As a consequence of such underlying similarities, the Flow Number U^* has similarities with the Karlovitz number that is employed in the correlations of premixtures. Also, just as normalised jet burner diameters, D/δ_k, can be correlated with U^*, in jet flame flows, in similar fashion normalised kernel diameters can be correlated with Karlovitz numbers in premixed flames. This joint applicability to both types of flame is demonstrated by Fig. 8 in [14]. A unifying aspect is not only flame quenching, but also its obverse, namely, flame initiation from an initial hot kernel of reacting gas.

The value of D has a dominant role on quench. Where it is small, in Fig. 1 at the top of the diagram, quenching is more probable. Where it is large, at the bottom of the diagram, there can be large, lifted, stable flames. Relative to most hydrocarbons, H_2 acts like a larger diameter flame, through its low flame thickness and low δ_k/D value. Although C_3H_8 is prone to leakages at small diameter holes, significantly smaller leakages are possible with H_2, because of its high diffusivity and reactivity, with a, uniquely small δ_k. Its flame is scarcely visible, making detection difficult. Possibly the weakest flame that has been subjected to analysis is the 0.46-watt H_2 leakage type flame, with a flow rate of 3.9 μg/s [15] on a 0.152 mm diameter hypodermic needle. In Fig. 1 its heat release rate and location are shown, with coordinates of approximately $U^*=0.5$, and $\delta_k/D=0.2$. An increase in flow rate might eventually lead to blow-off. This tiny flame contrasts nicely with the designed H_2 flaring from a nuclear reactor in [6], also shown in Fig 1.

4.2. (NH_3+H_2) flames

The contrasting locations of the (NH_3+H_2) points in the plots of Figs. 2 and 3 are noteworthy. In the former, the (NH_3+H_2) blow-off points are far removed from those of H_2. In contrast, in Fig. 3 the NH_3+H_2 points are much more closely related to the hydrocarbon points. The NH_3+H_2 blend has similar burning characteristics to a hydrocarbon, avoiding both the low burning characteristics of NH_3 and the fast burning H_2.

There is clearly a potential for practical (NH_3+H_2) and (NH_3+CH_4) gas turbine power generation. Developed powers of between 18.4 and 44.4 kW are reported in [16]. With NH_3+air, combustion efficiencies ranged from 89% to 96%. Supportive data on CH_4+NH_3 laminar burning velocities are available in [17].

In combination with Eq. (2), to evaluate (P_i/P_a), with the appropriate value of δ_k/D, a horizontal line drawn in Fig. 2 can represent an increasing fuel velocity, which is less than that for blow-off, and the velocity can be calculated up to that existing at blow-off.

5. Conclusions

1. The U^*-δ_k/D Blow-off diagram has been strengthened by the introduction of further data from new fuels, and further sampling of existing fuels.

2. Operational understanding of the practical behaviour of blended fuels, through experience with methane-hydrogen and ammonia-hydrogen blends has been improved.

3. Ammonia has become a successful fuel, when combined with hydrogen. Such blends can have similar heat release rates properties to conventional hydrocarbon fuels.

4. There is, however, a dearth of information on the NH_3+H_2 blends, particularly of different

blow- off diameters. More data over a range of $NH_3 + H_2$ blends are required, to make this plot more definitive.

5. Although energetically inefficient, there are advantages in hydrogen-ammonia as a fuel, their jet flames can blow-off at very low heat release rates.

6. There are large variations in the blow-off velocities of the different fuels.

7. The less reactive fuels blow-off more easily. The blow-off velocity can be indicative of the heat release rate of the fuel.

8. Flame extinction at jet flame blow-off is closely related to that observed for premixed turbulent flame kernels. As a consequence, U^*, has similarities with the Karlovitz number employed with premixtures.

This paper is based upon a presentation at the 10th International Seminar on Fire and Explosion Hazards in 2022 in Oslo [18].

References

[1] D. Bradley, P.H. Gaskell, X.J. Gu, A. Palacios, Jet flame heights, lift-off distances, and mean flame surface density for extensive ranges of fuels and flow rates, Combust. Flame. 164 (2016) 400–409. https://doi.org/10.1016/j.combustflame.2015.09.009

[2] C. Morley, GasEq. A chemical equilibrium program for windows (2005). htpp://www.gaseq.co.uk.

[3] J. Göttgens, F. Mauss, N. Peters, Analytic approximations of burning velocities and flame thicknesses of lean hydrogen, methane, ethylene, ethane, acetylene and propane flames, Proc. Combust. Inst. 24 (1992) 129–135. https://doi.org/10.1016/S0082-0784(06)80020-2

[4] A. Palacios, D. Bradley, Conversion of natural gas jet flame burners to hydrogen, Int. Jour. Hydrog. Energy. 46 (2021) 17051–17059. https://doi.org/10.1016/j.ijhydene.2021.02.144.

[5] A. Palacios, D. Bradley, Generalised correlations of blow-off and flame quenching for subsonic and choked jet flames, Combust. Flame. 185 (2017) 309–318. https://doi.org/10.1016/j.combustflame.2017.07.019

[6] A. Palacios, D. Bradley, Hydrogen generation, and its venting from nuclear reactors, Fire Saf. J. 113 (2020) 102968.

[7] D. Stamps, S. Tieszen, Blowout of turbulent jet diffusion flames, Fuel. 118 (2014) 113–122. https://doi.org/10.1016/S0082-0784(85)80515-4

[8] D.H. Um, J.M. Joo, S. Lee, O.C. Kwon, Combustion stability limits and NO_X emissions of non-premixed ammonia-substituted hydrogen-air flames, Int. J. Hydrog. Energy. 38 (2013) 14854–14865. https://doi.org/10.1016/j.ijhydene.2013.08.140

[9] H. Kobayashi, A. Hayakawa, K.D. Kunkuma, A. Somarathne, E.C. Okafor, Science and technology of ammonia combustion, Proc. Combust. Inst. 37 (2019) 109–133. https://doi.org/10.1016/j.proci.2018.09.029

[10] C. Lhuillier, P. Brequignya, N. Lamoureuxd, F. Continoe, C. Mounaim-Roussellea, Experimental investigation on laminar burning velocities of ammonia-hydrogen/air mixtures at elevated temperatures, Fuel. 263 (2020) 116653. https://doi.org/10.1016/j.fuel.2019.116653

[11] J.H. Lee, S.I. Lee, O.C. Kwon, Effects of ammonia substitution on hydrogen/air flame propagation and emissions, Int. J. Hydrog. Energy. 35 (2010) 11332–11341. https://doi.org/10.1016/j.ijhydene.2010.07.104

[12] H.B. Dixon, G. Greenwood, On the velocity of sound in mixtures of gases, Proc. R. Soc. A. 109 (1925) 561–569. https://doi.org/10.1098/rspa.1925.0145

[13] Aspen-Hysys V10®, 2021 Aspen Technology Inc. https:/-Home.aspentech.com/products/pages/new-in- aspen-plus.

[14] D. Bradley, M. Shehata, M. Lawes, P. Ahmed, Flame extinctions: critical stretch rates and sizes, Combust. Flame. 212 (2020) 459–468. https://doi.org/10.1016/j.combustflame.2019.11.013

[15] M.S. Butler, C.W. Moran, P.B. Sunderland, R.L. Axelbaum, Limits for hydrogen leaks that can support stable flame, Int. Jour. Hydrog. Energy. 34 (2009) 5174–5182. https://doi.org/10.1016/j.ijhydene.2009.04.012

[16] Osamu Kurata, Norihiko Iki, Takayuki Matsunuma, Takahiro Inoue, Taku Tsujimura, Hirohide Furutani, Hideaki Kobayashi, Akihiro Hayakawa, Performances and emission characteristics of NH3–Air and NH_3–CH_4 – Air combustion gas-turbine power generations, Proc. Combust. Inst. 36 (2017) 3351–3359. https://doi.org/10.1016/j.proci.2016.07.088

[17] C. Okafor, Y. Naito, S. Colson, A. Ichikawa, T. Kudo, A. Hayakawa, H. Kobayashi, Experimental and numerical study of the laminar burning velocity of CH_4-NH_3-Air premixed flames, Combust. Flame. 187 (2018) 185–198. https://doi.org/10.1016/j Combust.Flame.2017.09.002

[18] A. Palacios, D. Bradley, Longhua Hu, Blow-off of fuel jet flames in the atmosphere, Proceedings of the Tenth International Seminar on Fire and Explosion Hazards (ISFEH10), (2022) pp. 404–413. Edited by K. Vågsæther, A. W. Lach, D. Bradley, and J. Lundberg. Published by University of South-Eastern Norway.